

## SiC(0001): A surface Mott-Hubbard insulator

V. I. Anisimov, A. E. Bedin, and M. A. Korotin  
*Institute of Metal Physics, Ekaterinburg, GSP-170, Russia*

G. Santoro and S. Scandolo  
*International School for Advanced Studies (SISSA), Via Beirut 2, Trieste, Italy*  
*and Istituto Nazionale per la Fisica della Materia (INFM), Via Beirut 2, Trieste, Italy*

E. Tosatti  
*International School for Advanced Studies (SISSA), Via Beirut 2, Trieste, Italy;*  
*Istituto Nazionale per la Fisica della Materia (INFM), Via Beirut 2, Trieste, Italy;*  
*and International Centre for Theoretical Physics (ICTP), Trieste, Italy*

(Received 1 June 1999)

We present *ab initio* electronic structure calculations for the Si-terminated SiC(0001) $\sqrt{3}\times\sqrt{3}$  surface. While local-density approximation (LDA) calculations predict a metallic ground state with a half-filled narrow band, Coulomb effects, included by the spin-polarized LDA+ $U$  method, result in a magnetic (Mott-Hubbard) insulator with a gap of 1.5 eV, comparable with the experimental value of 2.0 eV. The calculated value of the intersite exchange parameter,  $J=30$  K, leads to the prediction of a paramagnetic Mott state, except at very low temperatures. The observed Si 2p surface core-level doublet can naturally be explained as an on-site exchange splitting.

The fractional adlayer structures on semiconductors show rich phase diagrams with potential instabilities of the charge-density-wave- (CDW) and spin-density-wave- (SDW) type at low temperatures, as well as Mott insulating phases.<sup>1</sup> The (0001) $\sqrt{3}\times\sqrt{3}$  surface of hexagonal SiC [as well as the closely analogous (111) $\sqrt{3}\times\sqrt{3}$  of cubic SiC] expected from standard LDA calculations to be a two-dimensional metal with a half-filled narrow band of surface states in the bulk energy gap<sup>2,3</sup> — is instead experimentally proven to be an insulator with a rather large (2.0 eV) band gap.<sup>4,5</sup> It has been suggested that this system is a Mott insulator<sup>6</sup> due to the large value of ratio  $U/W$ , where  $U$  is the Coulomb interaction parameter, of the order of several eV, and  $W$  is the surface bandwidth, calculated to be about 0.35 eV.<sup>2,3</sup> Very recent STM data further confirm this picture.<sup>7</sup> However, a detailed electronic description of the ensuing state and of its magnetic implications is not yet available.

Here we present an electronic structure calculation for this system, based on the LSDA+ $U$  Method,<sup>8</sup> which is able to take into account Coulomb interactions between localized electrons. The result—an insulating surface, with a large intra-adatom exchange splitting, but an exceedingly weak antiferromagnetic interadatom exchange coupling—is now in quantitative agreement with available photoemission data.

The generalized LSDA+ $U$  method<sup>9</sup> is devised to partially cure the weakness of the local spin-density approximation (LSDA) functional in dealing with interacting electrons in strongly localized orbitals, by supplementing the standard LSDA functional,  $E^{\text{LSDA}}[\rho^\sigma(\mathbf{r})]$  where  $\sigma=\uparrow,\downarrow$ , with a mean-field Hartree-Fock factorization  $E^U$  of the screened Coulomb interaction  $V_{\text{ee}}$  among electrons in localized atomic orbitals  $i,m$ . (Here  $i$  collectively labels the quantum number  $n$ , the angular momentum  $l$ , and the atomic site, while  $m$

labels the projection of the angular momentum.) The generalized LSDA+ $U$  functional is then written as

$$E^{\text{LSDA}+U} = E^{\text{LSDA}}[\rho^\sigma(\mathbf{r})] + \sum_i E^U[\{n^{i,\sigma}\}] - E_{\text{dc}}, \quad (1)$$

where  $n^{i,\sigma} = n_{mm}^{i,\sigma}$ , is the localized orbital occupation density matrix. Double counting of the localized orbital contribution to the energy, already included by LSDA in an average way, is taken into account in Eq. (1) by subtracting a compensating term

$$E_{\text{dc}} = \frac{1}{2} \sum_i \left[ UN_i(N_i - 1) - J \sum_\sigma N_i^\sigma(N_i^\sigma - 1) \right], \quad (2)$$

where  $U$  and  $J$  are the screened Coulomb and exchange parameters,<sup>10,11</sup>  $N_i^\sigma = \sum_m n_{mm}^{i,\sigma}$ , and  $N_i = N_i^\uparrow + N_i^\downarrow$ .

Minimization of this modified functional with respect to the charge density  $\rho^\sigma(\mathbf{r})$  and the orbital occupation  $n_{mm}^{i,\sigma}$ , leads to an effective single-particle Hamiltonian

$$\hat{H} = \hat{H}_{\text{LSDA}} + \sum_{i,\sigma} \sum_{mm'} |im\sigma\rangle V_{mm'}^{i,\sigma} \langle im'\sigma| \quad (3)$$

which corrects the usual LSDA potential through a localized orbital contribution of the form

$$\begin{aligned} V_{mm'}^{i,\sigma} = & \sum_{\{m\}} \{ \langle m,m'' | V_{\text{ee}} | m',m''' \rangle (n_{m''m''}^{i,\sigma} + n_{m''m''}^{i,-\sigma}) \\ & - \langle m,m'' | V_{\text{ee}} | m''',m' \rangle n_{m''m''}^{i,\sigma} \} \\ & - U(N_i - \frac{1}{2}) + J(N_i^\sigma - \frac{1}{2}). \end{aligned} \quad (4)$$

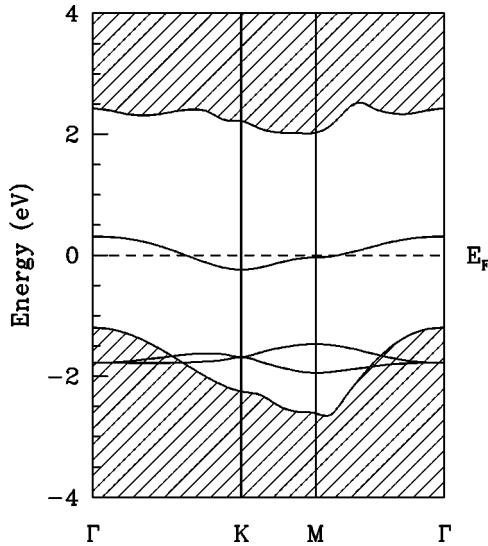


FIG. 1. Energy bands obtained from a standard LDA calculation for the SiC(0001) $\sqrt{3} \times \sqrt{3}$  surface. Brillouin-zone notations correspond to a unit cell with one Si adatom. Energy is measured from the Fermi level. Note the narrow half-filled surface band.

Important ingredients in the calculation are the matrix elements of screened Coulomb interaction  $V_{ee}$  that we parametrize, in analogy with the atomic case, in terms of effective Slater integrals  $F^k$  (Ref. 12) which, in turn, can be linked to the Coulomb and Stoner parameters  $U$  and  $J$ , as obtained from LSDA-supercell constrained calculations.<sup>11,13</sup> For Si, we apply the above corrections to  $3p$  states only, since  $3s$  states are fully occupied. The calculated Coulomb and Stoner parameters for Si  $3p$  states are  $U=8.6$  eV and  $J=1$  eV, respectively. The electronic structure calculations we have performed rely on the linear muffin-tin orbitals (LMTO) method,<sup>14</sup> and use the Stuttgart TBLMTO-47 code. An important point is that the calculation allows us, through the Green's-function method, to evaluate the effective intersite exchange interaction parameters  $J_{ij}$ , as second derivatives of the ground state energy with respect to the magnetic moment rotation angle.<sup>15,9</sup>

The SiC(0001) $\sqrt{3} \times \sqrt{3}$  surface was simulated by a slab containing two SiC bilayers plus a Si adatom layer. The Si adatoms were placed in the  $T_4$  positions of the upper (Si) surface. All atomic positions were fixed to the values calculated by Ref. 2. The bottom surface (C atoms of the fourth atomic layer) was saturated with hydrogen atoms. A standard LDA calculation for the  $\sqrt{3} \times \sqrt{3}$  unit cell containing one Si adatom gave, as expected, a metallic ground state with a half-filled narrow band situated within the energy gap of bulk SiC (Fig. 1). This surface band originates from the dangling bonds of the Si adatoms ( $p_z$  orbitals). The corresponding Wannier function, however, contains less than 50% of the adatom  $p_z$  orbitals, for, as is well known,<sup>2</sup> it extends itself down into the first SiC bilayer.

The LSDA+ $U$  method, relying on a Hartree-Fock-like mean-field approximation, can only deal with statically long-range-ordered ground states. It is generally believed<sup>16</sup> that a triangular lattice of electrons at commensurate filling, with nearest-neighbor hopping, and a strong Hubbard repulsion—i.e., in the Heisenberg limit—possesses, in spite of strong

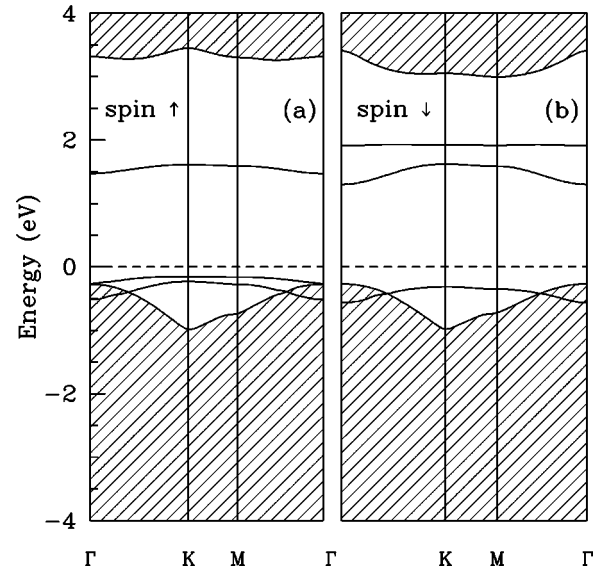


FIG. 2. LSDA+ $U$  energy bands for the spin-polarized collinear state of SiC(0001) $3 \times 3$  surface. Brillouin-zone notations correspond to the unit cell with three Si adatoms. (a) Spin-up electrons, (b) spin-down electrons. Energy is measured from the Fermi level. Note the insulating state, with a gap of about 1.5 eV.

quantum fluctuations, a three-sublattice  $120^\circ$  Néel long-range order—a commensurate spiral spin-density wave with  $120^\circ$  spins lying on a plane. This kind of noncollinear magnetic order can, in principle, be handled by LSDA+ $U$ , through a straightforward extension of the functional. However, that extension makes the scheme not only computationally heavier, but of intrinsically worse quality than the corresponding collinear calculation, as recently found in another case.<sup>17</sup> We therefore decided to carry out our calculation in the correct three-sublattice supercell (with three Si adatoms) but to restrict to collinear magnetic moments. Noncollinearity is then taken into account within a much less computationally heavy Hubbard model, the resulting small value of antiferromagnetic coupling further supporting the superior accuracy of this approach.

We started our LSDA+ $U$  calculation assuming two adatoms with a finite spin-up projection of the magnetic moment, and the third with spin down. The result converges to a stable magnetic insulating ground state with an energy gap of 1.5 eV, which compares rather well with the experimental value of 2.0 eV.<sup>5</sup> The corresponding energy bands are shown in Fig. 2. Of the three spin-up bands, two are occupied and one is empty [Fig. 2(a)], whereas for spin-down electrons [Fig. 2(b)] one band is occupied and two are empty. Consequently, there is a net magnetization corresponding to one spin for three adatoms. Of course, this net magnetic moment will disappear in the true noncollinear antiferromagnetic state (except perhaps for a small fraction which might be stabilized by surface spin-orbit coupling).

As a further check that the restriction to collinear spins does not really alter the main features of the bands in a substantial way, we performed a Hubbard model calculation for the possible  $3 \times 3$  magnetic phases, within a Hartree-Fock (HF) treatment.<sup>1</sup> Restricting ourselves to a one-band model with a nearest-neighbor hopping  $t \approx 0.04$  eV (as ex-

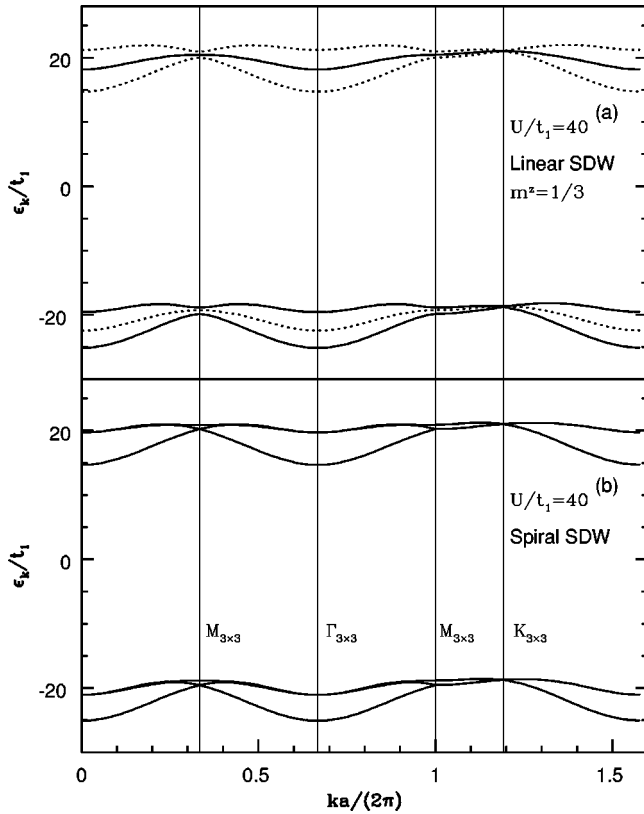


FIG. 3. Tight-binding HF electronic bands along high-symmetry directions of the Brillouin zone for the one-band Hubbard model at  $U_{\text{eff}}/t_1 = 40$  for the two magnetic solutions: (a) linear SDW with a net uniform magnetization  $m^z = 1/3$ ; (b) spiral SDW, with finite on-site magnetization, and  $m^z = 0$ . Solid and dashed lines denote up and down bands, respectively.

tracted from the LDA surface bandwidth), we use an effective Hubbard  $U$  roughly equal to the *ab initio* energy gap of  $\approx 1.5$  eV. The results for the two magnetic solutions found are shown in Figs. 3(a,b). Figure 3(a) shows the linear SDW solution with a uniform magnetization  $m^z = 1/3$ , which compares rather well with the *ab initio* surface bands. Allowing for noncollinear spins, we then obtain the spiral SDW solution whose bands are shown in Fig. 3(b). We stress the fact that the spiral SDW is the actual HF ground state, while the linear SDW is only a metastable state. We note, however, that the ground-state energies of the two solutions differ by less than 0.5 meV/adatom, so that unrealistically precise *ab initio* calculations would be necessary to decide which of the two is the actual ground state. Moreover, the HF bands for the two solutions are rather similar, apart from some extra splittings introduced by the collinear magnetic solution. It is not clear whether the present resolution of photoemission data<sup>4,5</sup> would allow us to distinguish between these two slightly different sets of bands.

Coming back to the *ab initio* study, we have calculated a magnetic moment for the Si adatom of approximately  $0.6\mu_B$ . This reduction is, of course, not due to quantum fluctuations, absent in the LSDA+ $U$ , but to the subsurface delocalization of the Wannier function, whose weight is only about half on the Si adatom. For the same reason, the energy-gap value of 1.5 eV is roughly 4–5 times smaller than the

bare  $U$  value. In fact, the LSDA+ $U$  correction to the potential of a particular orbital  $m\sigma$  is roughly proportional to  $U(1/2 - n_{m\sigma})$ , and the splitting of the potentials for spin-up and spin-down  $p_z$  orbitals of Si adatoms is proportional to the magnetic moment on the adatom. This means that this potential splitting can be estimated to be roughly  $U/2$ . If one takes into account that the potential correction is applied to the Si  $3p$  orbital, which is about one-half of the total Wannier function corresponding to the half-filled band, its effect on the energy splitting  $\Delta E$  will be further reduced by a factor two, yielding roughly  $\Delta E \approx U/4$ , close to the value obtained in our actual LSDA+ $U$  calculation.

We have also calculated the value of the intersite exchange parameter  $J_{ij}$  corresponding to the interaction between the spins of the electrons localized on neighboring Si adatoms, and obtained a value of  $J_{ij} = 30$  K. The corresponding one-band Hubbard model estimate is  $J_{ij} = 4t^2/U_{\text{eff}}$ , where  $t$  is the nearest-neighbor hopping parameter and  $U_{\text{eff}}$  is the effective Coulomb Hubbard  $U$ . Taking  $U_{\text{eff}}$  of the order of the energy gap ( $\approx 2$  eV) and  $t = 0.04$  eV, we obtain 37 K, which agrees quite well with the LSDA+ $U$  result.

The existence of finite magnetic moments on the Si adatoms should be experimentally detectable. Methods which require magnetic long-range order do not seem viable, since the only circumstance where a finite-temperature order parameter could survive in this frustrated 2D magnetic system would be in the presence of a large spin-orbit-induced magnetic anisotropy favoring out-of-surface ordering, which we do not have reason to expect. Therefore, without ruling out the possibility of low-temperature ordering, we believe that the SiC(0001) $\sqrt{3} \times \sqrt{3}$  surface will be in an overall paramagnetic Mott insulating state, in spite of the existence of an on-site moment, at least down to liquid-nitrogen temperature.

The situation is much more promising at the intra-atomic level. Here, exchange splittings in the Si adatom  $2p$  core levels should be large and detectable. One complication is that the adatom dangling bond has a predominant  $3p_z$  character, which breaks the core-level symmetry between  $2p_z$  and  $2p_{x,y}$  by an amount not negligible in comparison to spin-orbit coupling and exchange. The  $2p$  core hole will exhibit a six-fold multiplet resulting from the joint effect of intra-atomic exchange, asymmetry, and spin orbit. An estimate for the multiplet splitting is obtained by assuming the valence electrons to be distributed with weights  $\alpha$  in  $3p_z\uparrow$ , and  $\beta/4$  in each  $3p_{x,y}\uparrow\downarrow$ . For  $\lambda_{\text{SO}} = 0$ , we calculate a bare asymmetry splitting  $\Delta = \epsilon_{2p_{x\uparrow}} - \epsilon_{2p_{z\uparrow}} = \alpha[(J_{zz} - J_{zx}) - (K_{zz} - K_{zx})] + (\beta/4)[2(K_{zz} - K_{zx}) - (J_{zz} - J_{zx})]$ , where  $K_{zz(x)} = (2p_{z(x)}, 3p_z|e^2/|\mathbf{r}_1 - \mathbf{r}_2||2p_{z(x)}, 3p_z)$  and  $J_{zz(x)} = (2p_{z(x)}, 3p_z|e^2/|\mathbf{r}_1 - \mathbf{r}_2||3p_z, 2p_{z(x)})$  are Coulomb and exchange integrals. The first square bracket dominates, and is estimated by a Si<sup>+</sup> Hartree-Fock calculation to be about 1 eV, so that  $\Delta \approx \alpha$  (eV). Since only about 50% of the dangling-bond orbital is  $3p_z$ , we obtain the desired crude estimate  $\Delta \approx 0.5$  eV. Exchange splittings are large for the  $2p_z$  case and small for the  $2p_{x,y}$ , reflecting the large differences in the corresponding exchange integrals  $J_{zz}$  and  $J_{zx}$ . When we include the spin-orbit interaction  $\lambda_{\text{SO}}\mathbf{L} \cdot \mathbf{S}$ , the final core hole levels are obtained as in Fig. 4. For  $\lambda_{\text{SO}} = 0.4$  eV we find a roughly three-peaked structure, the broad central peak four times as strong as each side peak. This offers an

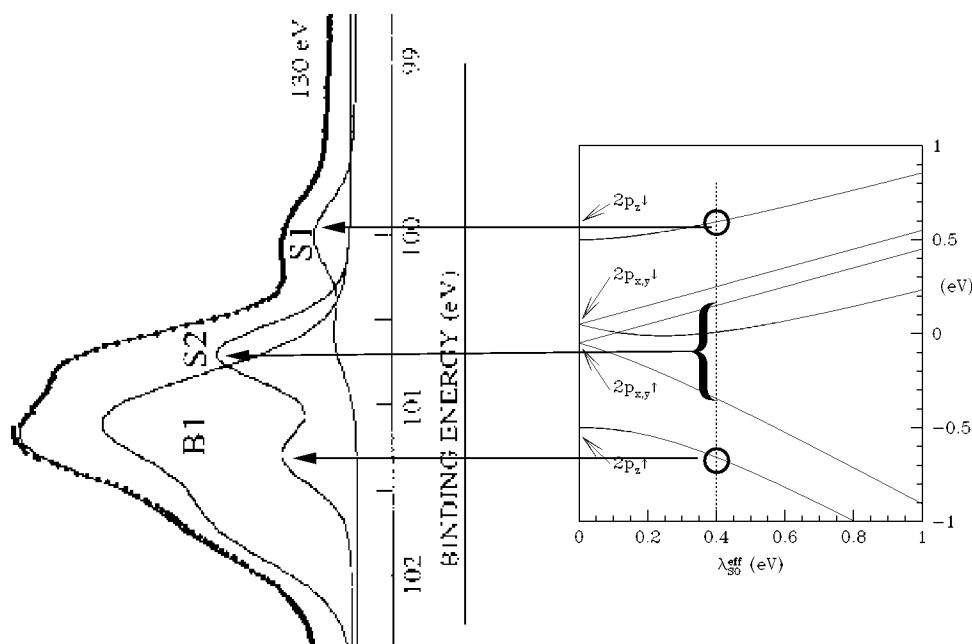


FIG. 4. Si  $2p$  core levels calculated as a function of spin-orbit coupling, in comparison with photoemission data and original fitting in terms of bulk ( $B1$ ) and two surface sites  $S1$  and  $S2$  by Johansson *et al.* (Ref. 18). Upon inclusion of intra-atomic exchange splitting the whole surface contribution  $S1 + S2$  can be explained as due to a single site.

alternative explanation of the experimental line shape<sup>18</sup> (see Fig. 4) in terms of a single exchange-split multiplet, rather than two chemically inequivalent sites  $S_1$  and  $S_2$  (Ref. 18) whose existence is otherwise not supported.

Additional direct experimental evidence for the Mott-Hubbard state could be obtained by a careful study of adatom ( $3p_z$ ,  $3p_z$ ) Auger spectral intensities, which should be easily singled out owing to the large gaps. The probability of double occupancy of the adatom dangling-bond orbital should be almost completely suppressed, dropping from the band value of  $1/4$  to a value of order  $t/U$  which is one order of magnitude smaller. Even considering that only half of the orbital is adatom  $3p_z$ , this surface should show a ( $3p_z$ ,  $3p_z$ )

Auger intensity which, by comparison with the remaining ( $3p_x, 3p_y$ ) values, is anomalously small, as a proof of its Mott-Hubbard state.

More experimental and theoretical effort is clearly called for to check these strong correlations and related magnetic effects, possibly the first of this magnitude to be suggested for an sp-bonded, valence semiconductor surface.

We thank S. Modesti for useful discussions. Work at SISSA was partially supported by INFN through PRA LOTUS and HTSC, by MURST through COFIN97, and by the EU, through Contracts No. ERBCHRXCT940438 and No. FULPROP ERBFMRXCT970155. Work at IMP was supported by the Russian Foundation for Basic Research under Grant No. RFFI-98-02-17275.

<sup>1</sup>G. Santoro, S. Sorella, F. Becca, S. Scandolo, and E. Tosatti, *Surf. Sci.* **402–404**, 802 (1998); G. Santoro, S. Scandolo, and E. Tosatti, *Phys. Rev. B* **59**, 1891 (1999).

<sup>2</sup>J. E. Northrup and J. Neugebauer, *Phys. Rev. B* **52**, R17001 (1995).

<sup>3</sup>M. Sabisch, P. Kruger, and J. Pollmann, *Phys. Rev. B* **55**, 10561 (1997).

<sup>4</sup>L. I. Johansson *et al.*, *Surf. Sci.* **360**, L478 (1996).

<sup>5</sup>J.-M. Themlin, I. Forbeaux, V. Langlais, H. Belkhir, and J.-M. Debever, *Europhys. Lett.* **39**, 61 (1997).

<sup>6</sup>J. E. Northrup and J. Neugebauer, *Phys. Rev. B* **57**, R4230 (1998).

<sup>7</sup>V. Ramachandran and R. M. Feenstra, *Phys. Rev. Lett.* **82**, 1000 (1999).

<sup>8</sup>V. I. Anisimov, J. Zaanen, and O. K. Andersen, *Phys. Rev. B* **44**, 943 (1991); V. I. Anisimov, F. Aryasetiawan, and A. I. Liechtenstein, *J. Phys.: Condens. Matter* **9**, 767 (1997).

<sup>9</sup>A. I. Liechtenstein, J. Zaanen, and V. I. Anisimov, *Phys. Rev. B* **52**, R5467 (1995).

<sup>10</sup>O. Gunnarsson, O. K. Andersen, O. Jepsen, and J. Zaanen, *Phys. Rev. B* **39**, 1708 (1989).

<sup>11</sup>V. I. Anisimov and O. Gunnarsson, *Phys. Rev. B* **43**, 7570 (1991).

<sup>12</sup>B. R. Judd, *Operator Techniques in Atomic Spectroscopy* (McGraw-Hill, New York, 1963).

<sup>13</sup>V. I. Anisimov, I. V. Solovyev, M. A. Korotin, M. T. Czyzyk, and G. A. Sawatzky, *Phys. Rev. B* **48**, 16929 (1993).

<sup>14</sup>O. K. Andersen, *Phys. Rev. B* **12**, 3060 (1975).

<sup>15</sup>A. I. Liechtenstein, M. I. Katsnelson, V. P. Antropov, and V. A. Gubanov, *J. Magn. Magn. Mater.* **67**, 65 (1987).

<sup>16</sup>B. Bernu, C. Lhuillier, and L. Pierre, *Phys. Rev. Lett.* **69**, 2590 (1992); L. Capriotti, A. Trumper, and S. Sorella, *ibid.* **82**, 3899 (1999).

<sup>17</sup>R. Gebauer *et al.* (unpublished).

<sup>18</sup>L. I. Johansson, F. Owman, and P. Martensson, *Phys. Rev. B* **53**, 13793 (1996).